29p

UNPUBLISHED PRELIMINARY DATA

NSG-31-60

N65-88632

JET FLOW AND JET NOISE [redacted]

by

Erik Mollo-Christensen

Massachusetts Institute of Technology

29

Summary

The flow and sound fields of jets have been investigated experimentally. The information given in the paper includes examples of shadowgraph pictures, Mach-number profiles, pressure space-time correlations and spectra in the near field and spectra in the far field. Some consequences of the results are discussed.

1. Introduction

There is not much hope for a better theory of jet noise than Lighthill's theory (1,2,3) as elaborated upon by Ribner (4) and Williams (5).

This does not mean that the theory now available completes our detailed understanding of jet noise. It is rather that the problem beyond the present level of understanding is intractable and therefore, perhaps, uninteresting to theoreticians. In addition, our present understanding of jet noise has contributed significantly to the technology of jet noise prevention.

Whether our present knowledge and understanding is satisfactory or not depends upon one's purpose. Also, of course, we don't know how good the present theory is, because it is as good as most present experimental information, in the sense that when experiment and theory have disagreed in the past, it has been difficult to decide which to blame. Among the reasons for this, one can mention that the experiments are difficult to perform accurately under controlled circumstances, and that a theory for a stochastic process can yield the correct root mean square without being physically correct.

For the last few years, we have been making measurements of jet noise at M.I.T. with the hope of learning more about the phenomenon and the theory. An important additional consideration was the fact

that while the theories give methods for predicting the far field noise in terms of velocity fluctuations, they say very little about how to determine the velocity fluctuations. This may not be serious, since the similarity laws governing incompressible jet turbulence are known (6), but our curiosity went beyond similarity. I shall here give a short description of our measurements and some examples of our results. The detailed results will be published elsewhere.

2. The experimental arrangement.

In the construction of the apparatus, extreme care was taken to avoid parasitic sources of noise and vibration. After completion of the apparatus, it took us a year of modification and rebuilding before we got data which obeyed the more obvious similarity laws for changes of scale and flow variables. The arrangement is shown in Fig. 1. In the settling chamber, the air passes through steel wool pads, a long honeycomb and screens, and the area ratio of nozzle area to settling chamber cross-section is either 1/144 or 1/720, depending upon the nozzle diameter. The rms turbulence level at the nozzle exit could not be detected using hot wire equipment which had a noise level of less than 10^{-5} as measured in terms of mean stream velocity. The anechoic chamber was designed for short wavelengths, and worked satisfactorily.

Among the parasitic influences, which gave trouble before they were eliminated, were: vibrations from the air supply, amplifier microphonics, sound-induced vibrations of the microphone supports,

scattering around cables and microphone supports, besides many others, adding up to a long tale of extended frustration, which will not be told here.

3. Flow observations

In this section we show the results of measurements obtained by Kolpin (16), his results will be published in detail elsewhere.

Figures 2 and 3 show shadowgraphs of the flow from nozzles of 1/2 inch and 1 inch diameter, operating at Mach number M = .6 and .8, respectively. The boundary layer on the nozzle wall at the exit is laminar in Fig. 2, while it is transitional or turbulent in Fig. 3.

Figure 4 shows the local Mach number M(x,y) as a function of distance from the nozzle exit plane $x = \xi \cdot d$ and distance from the jet axis y. The similarity when $(M/M_{centerline})$ is plotted versus $\eta = \frac{y - (d/2)}{d/2}$ is shown in the lower half of Fig. 4.

The laminar core extends approximately four diameters downstream of the nozzle exit for the larger jet (d = 1") and six diameters downstream for the smaller jet (d = 1/2"), independent of exit Mach number. The flow in the smaller jet was laminar at the nozzle exit.

The root mean square fluctuation of axial velocity $\tilde{u}/U_{centerline} = \sqrt{u'^2}/U_{c.l.}$ at y = d was found to be practically constant for distances from the nozzle exit plane between $1 < \frac{x}{d} < 6$ for both jets, $\tilde{u}/U_{centerline}$ varying between .10 and .12. Figure 5 shows the normalized power spectral density of these velocity fluctuations, u' at $\xi = \frac{x}{d}$,

$\frac{y}{d/2} = 1$, versus dimensionless frequency $\omega x/U_{exit}$, as measured by Kolpin (16). The normalization is such that $\int_0^\infty \phi(\omega)\, d\omega = 1$ Finally, Fig. 6 shows the space-time correlation coefficient of axial velocity fluctuations obtained for one combination of flow parameters. The correlation coefficient $R_{uu}(\xi, \Delta\xi, \tau)$ is defined as

$$R_{uu}(\xi, \Delta\xi, \tau) = \frac{\langle u'(\xi, t)\, u'(\xi + \Delta\xi, t+\tau)\rangle}{\tilde{u}(\xi)\quad \tilde{u}(\xi + \Delta\xi)}$$

Figure 6 shows curves representing the variation of R_{uu} with delay time τ for various values of $\Delta\xi$, measured at $y = d/2$, $M_{exit} = .3$ for a nozzle of one inch diameter. The logarithmic decrement distance $\Delta\xi$ for which R_{uu} is reduced by a factor of 1/e is approximately $\Delta\xi = \Delta x/d = 1$

The rounding off of the curves with increasing $\Delta\xi$ represents the rapid decay of the small eddies, while the larger eddies endure for a longer distance.

The speed of travel of the disturbances (correlation speed) was found to be $U_{exit}/2$ within the limits of experimental accuracy. These flow data are insufficient for predicting the sound emitted from the jet, although the data appear to support many of the assumptions usually made as to persistence, scale and similarity of velocity fluctuations. The data also agree with those obtained by previous investigators (Corrsin (8), Corrsin and Kistler (7), Corrsin and Uberoi (8), Crane and Pack (10), Kanpur (11), Laurence (12), Lassiter (13), Liepmann and Laufer (14) Morkovin (15),

although the present data are more complete as far as compressible jet flows are concerned.

4. Pressure field measurements

Using small microphones of our own construction, we measured the pressure fluctuations near the jet and power spectral densities and space-time correlations. Figure 7 shows the microphone arrangement for near field measurements. The microphone support, a combination of steel, brass, foam rubber and torturous shapes of styrofoam, was the successful result of time-consuming and perhaps not fully rational experimentation.

Because near field pressure measurements have in the past been suspect because of the possibility of gusts hitting the microphone, one needs to discuss this point.

There are always gusts on a microphone near a jet since the unsteady velocity field extends to infinity. A microphone not in the far field will be subject to "pseudo sound," the unsteady pressure field associated with turbulence moving past the microphone. If the presence of the microphone changes these pressure fluctuations noticeably, one may say that gusts are hitting the microphone. Since the problem of gusts is one of degree rather than of kind, we devised an ad hoc definition.

A human hair was glued to the side of the microphone, jutting out approximately one millimeter beyond its face. The hair was observed through a microscope at 20 times magnification. If the

hair appeared to move at all, we said there were gusts on the microphone. There were no gusts on the microphone in the results we are showing here.

The microphone responds to pressure fluctuations on its surface, this pressure depends upon the fluctuating velocity field at and away from the microphone. If the pressure fluctuations are small, one may find a linear superposition of pressure fields satisfactory, and the pressure fluctuation p' at a point x may be written as an integral over space and time of an operator on the field of velocity fluctuations

$$p'(\underset{\sim}{x},t) = -\int_{-\infty}^{t_1=t} \iiint_{V} G(\underset{\sim}{x},t\,|\,\underset{\sim}{y},t_1)\ \frac{\partial^2 (\rho u_i u_j)'}{\partial y_i\,\partial y_j}\,d\underset{\sim}{y}\,dt_1$$

where the prime denotes the time-dependent part. The approximations involved here is that viscous stresses do not affect the pressure-velocity relationship, and that the pressure density relationship is locally polytropic.

A microphone, therefore, responds to the entire velocity field. The Green's function $G(x,t\,|\,y,t)$ is, however, singular at $\underset{\sim}{x} = \underset{\sim}{y}$, $t = t_1$. One must therefore expect that velocity fluctuations near the microphone will affect the pressure at the microphone more than the same velocity fluctuation at a point far away.

As used in the near field, a microphone will respond to the more coherent part of the velocity field in its vicinity. Keeping this in mind, we may proceed to examine some of the results.

Figure 8 shows the root mean square amplitude of pressure fluctuations $\tilde{p}(\xi, \vartheta)$. The distance from the nozzle exit plane is $x = \xi \cdot d$, and ϑ is the semi-vertex angle of a right circular cone through the microphone and the nozzle edge, as shown in the figure. This variation is typical for both nozzles and all Mach numbers less than unity. The sensitive area of the microphone had a diameter of less than 1.5 millimeter. A set of typical spectra are shown in Fig. 9. The power spectral density of $p'(x,t)$ is plotted versus reduced frequency $S = \frac{\omega x}{2\pi U_{exit}}$ for several streamwise locations. Similarity appears to establish itself after transition has been completed. For high frequencies, the power spectral density decreases approximately as $(\frac{\omega x}{2\pi U_{exit}})^{-1/3}$. The spectra have a maximum near $\frac{\omega x}{2\pi U_{exit}} = .25$, the maximum value slowly decreasing with streamwise distance from the nozzle exit.

Examples of measured pressure space-time correlations are shown in Fig. 10 and 11. The cross-correlation coefficient $R_{pp}(\xi, \Delta\xi, \tau)$ is what is actually shown, plotted as curves for constant $\Delta\xi$.

R_{pp} is defined as follows:

$$R_{pp}(\xi, \Delta\xi, \tau) = \langle p'(\xi, t)\, p'(\xi + \Delta\xi, t + \tau) \rangle \Big/ \tilde{p}(\xi)\tilde{p}(\xi + \Delta\xi)$$

The data shown are raw data, taken directly from the output plotter of our correlator. One sees from the figures that one may wish to make a distinction between correlation phase velocity, W_{ph}, and

the velocity of the maximum correlation W_g. W_{ph} may be defined as

$$W_{ph} = W_{ph}(\Delta\xi) = \left(- \frac{\partial R_{pp}}{\partial \tau} \Big/ \frac{\partial R_{pp}}{\partial \xi} \right)_{R_{pp} = 0}$$

This velocity is in all our measurements found to differ by less than ten per cent from $U_{centerline}/2$. The microphones are therefore observing the pressure fluctuations associated with moving turbulence, rather than sound. An upstream source of noise could easily radiate enough sound to obscure what we measured, or at least change the correlation speed significantly.

The other correlation velocity, W_g, is more difficult to define, and I may be wrong in thinking of it as a group velocity. However, remembering that the mean flow in the jet is unstable, it is not surprising that one disturbance excites a few more of the same kind, these being added as the initial disturbance is propagating downstream. A jet flow also has a definite starting region, and develops fully within a few length scales from this region; the presence of a standing part of the disturbances is thus not surprising.

This is true in the sense of an average over a limited domain, as, for example, defined by the velocity field "seen" by a microphone. To a lesser degree, it also holds for local velocity correlations, as can be seen from Fig. 6. A crude approximation for the "large eddy" part of the near pressure field is the form:

$$R_{pp}(\xi, \Delta\xi, \tau) = \exp\left\{\left(-\frac{\Delta\xi}{l\cdot\xi}\right)+\left[\left(\Delta\xi - W_g\tau\right)/\sigma(\xi)\right]^2\right\}$$

$$\cdot \cos\left[\frac{\omega U_{exit}}{d}\left(\frac{\Delta\xi - W_{ph}\tau}{\xi}\right)\right]$$

where l is a decay distance, U/d a frequency parameter and σ a nondimensional disturbance length. Our measurements indicate that $W_g > W_{ph}$.

Figure 12 shows how the maximum pressure correlation decreases with separation $\Delta\xi$. The indicated persistence of the coherent part of the velocity field is indeed surprising, the distance for a decay by a factor of 1/e being typically of order two jet diameters and more than twice the distance of the upstream microphone from the nozzle exit.

Figures 13 and 14 show examples of the maximum pressure correlation coefficient across a jet diameter ($\alpha = 180^\circ$) and around one quarter of the jet circumference ($\alpha = 90^\circ$), respectively.

Again, the high correlation is remarkable, illustrating how the microphones respond to the more coherent part of the turbulent velocity correlations. Also notable is the increase in correlation with streamwise location, once the exit Mach number is above 0.3.

I do not understand why the Mach number enters in here, independently of jet diameter. The only reason I can think of is that

for as quiet upstream conditions as we had in our experiment, sound or compressibility plays a role in the transition processes in the jet. How important compressibility is in this respect is solely a function of the external noise and turbulence levels.

As a last example of the results obtained in our experiments, we show the far field spectra obtained at $M_{exit} = 0.8$ for jet diameters 1/2" and 1" (Fig. 15). The square root of the dimensionless power spectral density $\varphi\left(\frac{\omega d}{2\pi U_{exit}}\right)$ is plotted versus $\frac{\omega d}{2\pi U_{exit}}$ for several values of ϑ and distances r from the center of the nozzle opening. φ is defined by:

$$\left[\tilde{p}(r,\vartheta)\right]^2 = \left(\frac{\rho}{2} a^2 M^2\right)^2 \frac{d^2}{r^2} \int_0^\infty \varphi\left(\frac{\omega d}{2\pi U}\right) d\left(\frac{\omega d}{2\pi U}\right)$$

where ρ and a are density and speed of sound at the nozzle exit, respectively.

The power spectral densities differ for the two jet diameters, no simple M^n law describe the data within experimental accuracy, although for $\tilde{p}$ in the far field one finds that M^n fits if one let n vary from 9 to 6.7, which brackets M^8 rather neatly.

It appears possible to fit the spectra for $\vartheta > 60^\circ$ into some kind of similarity relationship, while the spectra for $\vartheta < 60^\circ$ are more complicated than the examples given by, for example, Ribner (4).

5. Conclusions

The pressure space-time covariance in the near field of a jet extends over several wavelengths of the sound emitted at the maximum of far field power spectral density.

The high-frequency space-time correlation decay fast with correlation distance, although it has not been measured in terms of decay per wavelength of emitted sound. More measurements are necessary.

The details of transition in a jet in the absence of upstream noise depends upon Mach number. The far field sound spectra from jets depend upon the details of the transition process as well as the structure of the fully developed turbulent jets.

None of these conclusions will affect the present methods for crude estimates of jet noise, the largest effect measured being less than ten decibels in power spectral density.

6. Acknowledgement

This work was supported by the National Aeronautics and Space Administration under Grant NsG 31-60.

The author wishes to acknowledge the contributions of his co-workers, M.A. Kolpin, J. Martuccelli and F. Merlis, whose efforts made the work possible.

References

1. Lighthill, M.J., On Sound Generated Aerodynamically - Part I - General Theory, Proceedings, Royal Society of Aeronautics, Vol. 211, pp. 564-587, 1952.
2. Lighthill, M.J., On Sound Generated Aerodynamically - Part II - Turbulence as a Source of Sound, Proceedings, Royal Society of Aeronautics, Vol. 222, pp. 1-32, 1954.
3. Lighthill, M.J., Sound Generated Aerodynamically, The Bakerian Lecture, 1961, published by Royal Aircraft Establishment, as Report Dir. 8 (November 1961).
4. Ribner, H.S., Aerodynamic Sound from Fluid Dilatations—A Theory of the Sound from Jets and Other Flows, Institute of Physics, University of Toronto, July 1962, UTIA Rept. No. 86 (AFOSR TN 3430).
5. Williams, J.E. Ff., "Noise from Convected Turbulence" 62nd Meeting, Acous. Society of America, Cincinnati, November 8-11, 1961.
6. Corrsin, S., Investigation of Flow in an Axially Symmetrical Heated Jet of Air, NACA Wartime Report No. W. 94, (ACR 3123).
7. Corrsin, S. and Kistler, A.L., Free Stream Boundaries of Turbulent Flows, NACA Report 1244.
8. Corrsin, S. and Uberoi, M., Further Experiments on the Flow and Heat Transfer in a Heated Turbulent Air-Jet, NACA TN No. 1865.
9. Corrsin, S. and Uberoi, M., Spectra and Diffusion in a Round Turbulent Jet, NACA Report No. 1040.
10. Grane, L.J. and Pack, D.C., The Laminar and Turbulent Mixing of Jets of Compressible Fluid, Part I - Flow Far From the Orifice, Journal of Fluid Mechanics Vol. 2, No. 5, pp. 449-455, 1957.
11. Kanpur, J.N., Transverse Component of Velocity in a Plane Symmetrical Jet of a Compressible Fluid, Quarterly Journal Mech. Applied Mathematics, Vol. II, No. 4, pp. 423-426, November 1958.
12. Laurence, J.C., Intensity, Scale and Spectra of Turbulence in Mixing of Free Subsonic Jet, NACA Tech. Report 1292, April 1956.

13. Lassiter, L.W., Turbulence in Small Jets at Exit Velocities up to 705 ft/sec, Journal of Applied Mechanics, Vol. 24, pp. 349-354, September 1957.

14. Liepmann, H.W. and Laufer, J., Investigation of Free Turbulent Mixing, NACA TN 1257, 1947.

15. Morkovin, Mark V., Note on Turbulence in Small Air-Jets at Exit Velocities up to 705 Feet Per Second, Journal of Applied Mechanics, Vol. 25, June 1958.

16. Kolpin, M.A., Flow in the Mixing Region of a Jet. National Aeronautics and Space Administration Grant NsG-31-60, ASRL TR 92-3, June 1962.

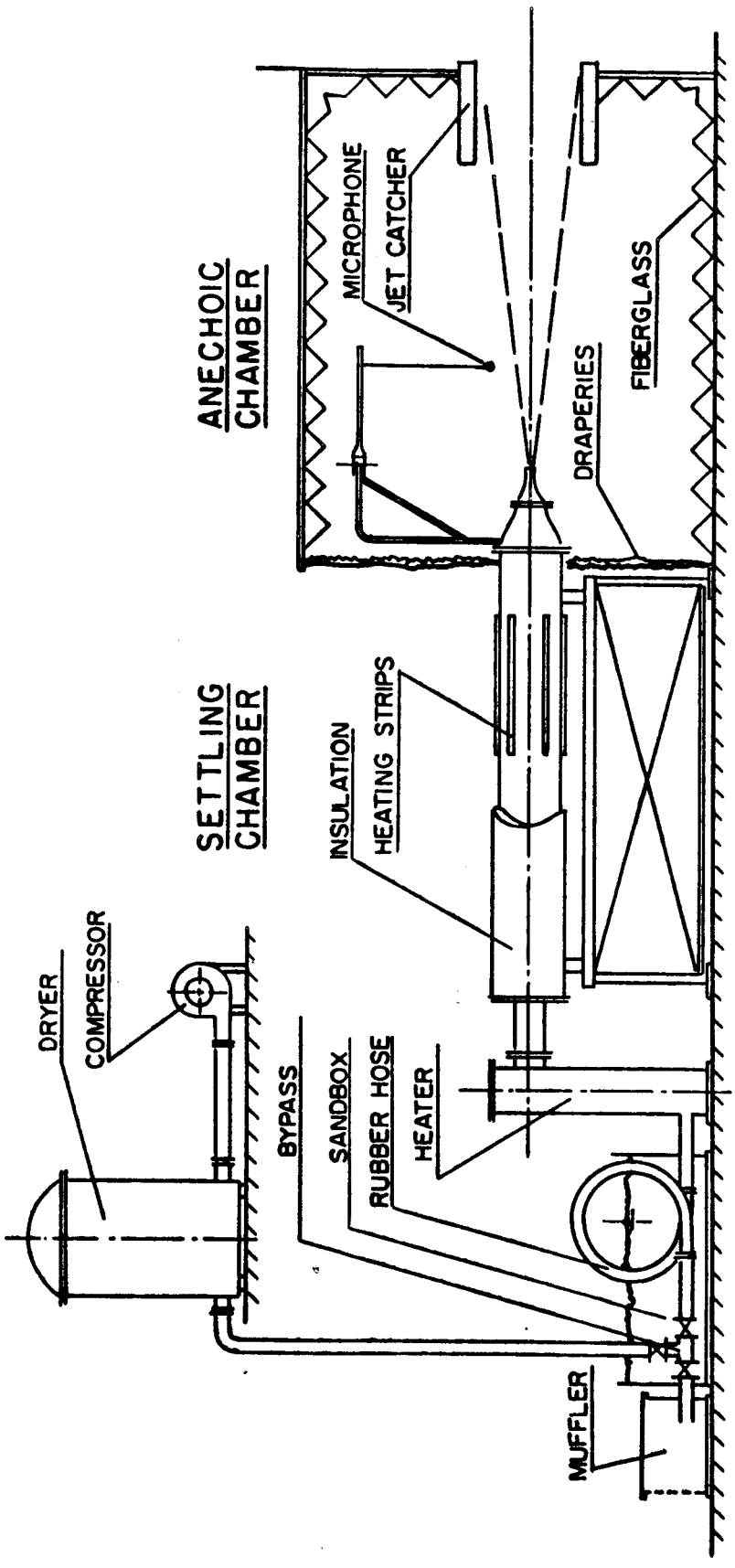

Figure 1. Experimental Arrangement

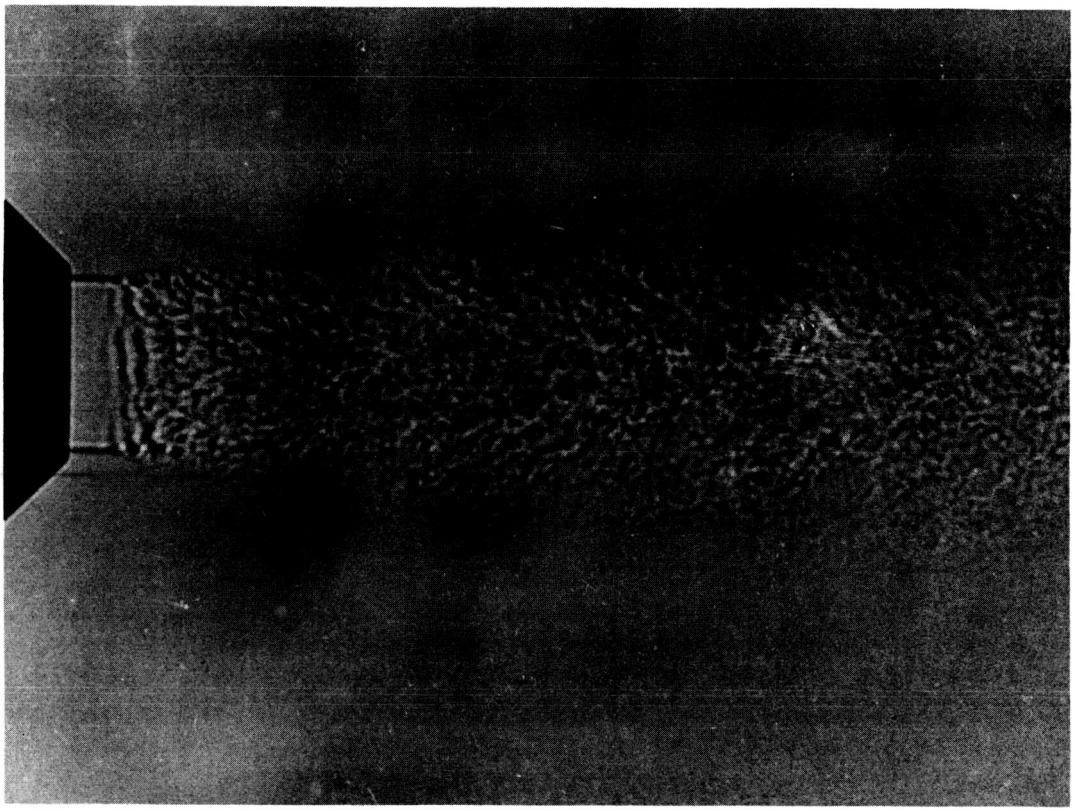

Figure 2. Shadowgraph D = $\frac{1}{2}$" , M = .6.

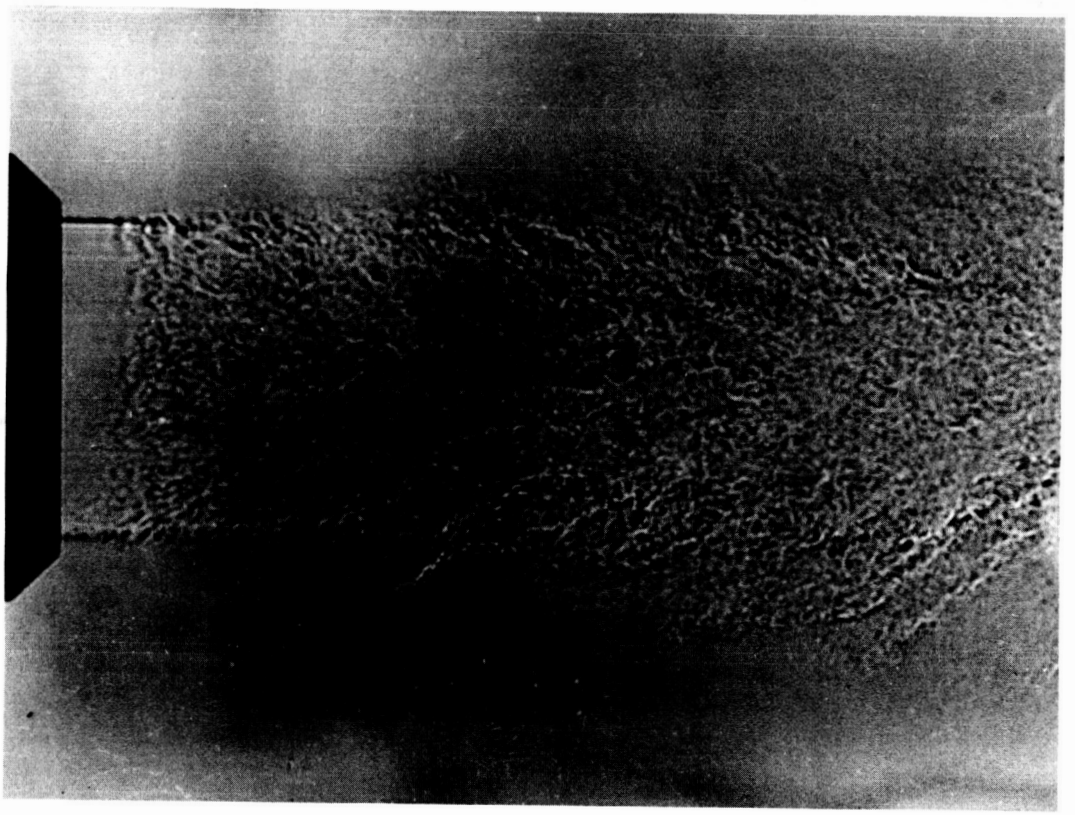

Figure 3. Shadowgraph D = 1" , M = .8.

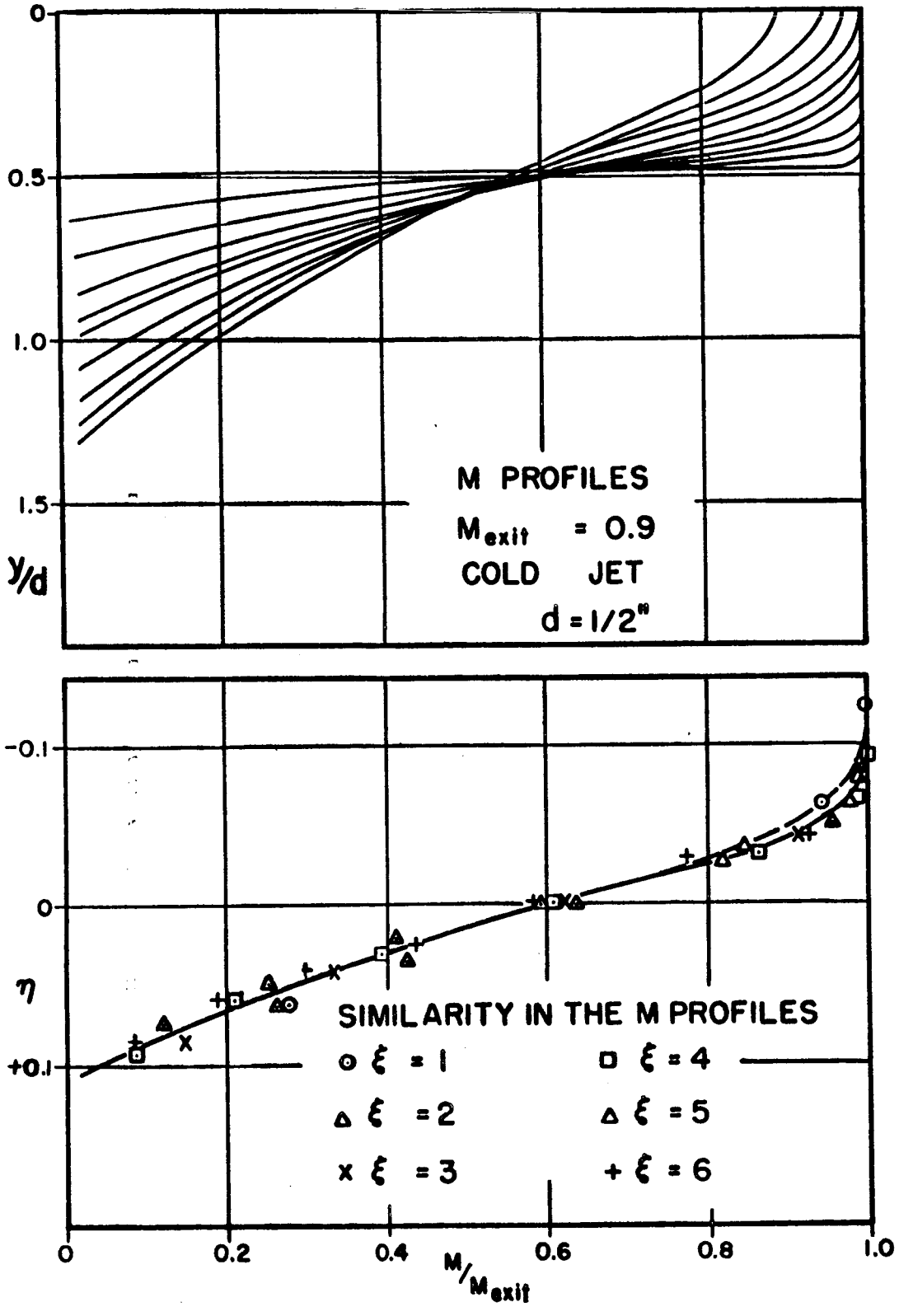

Figure 4. Variation of Mach numbers with distance from nozzle exit plane (x) and distance from jet axis (y).

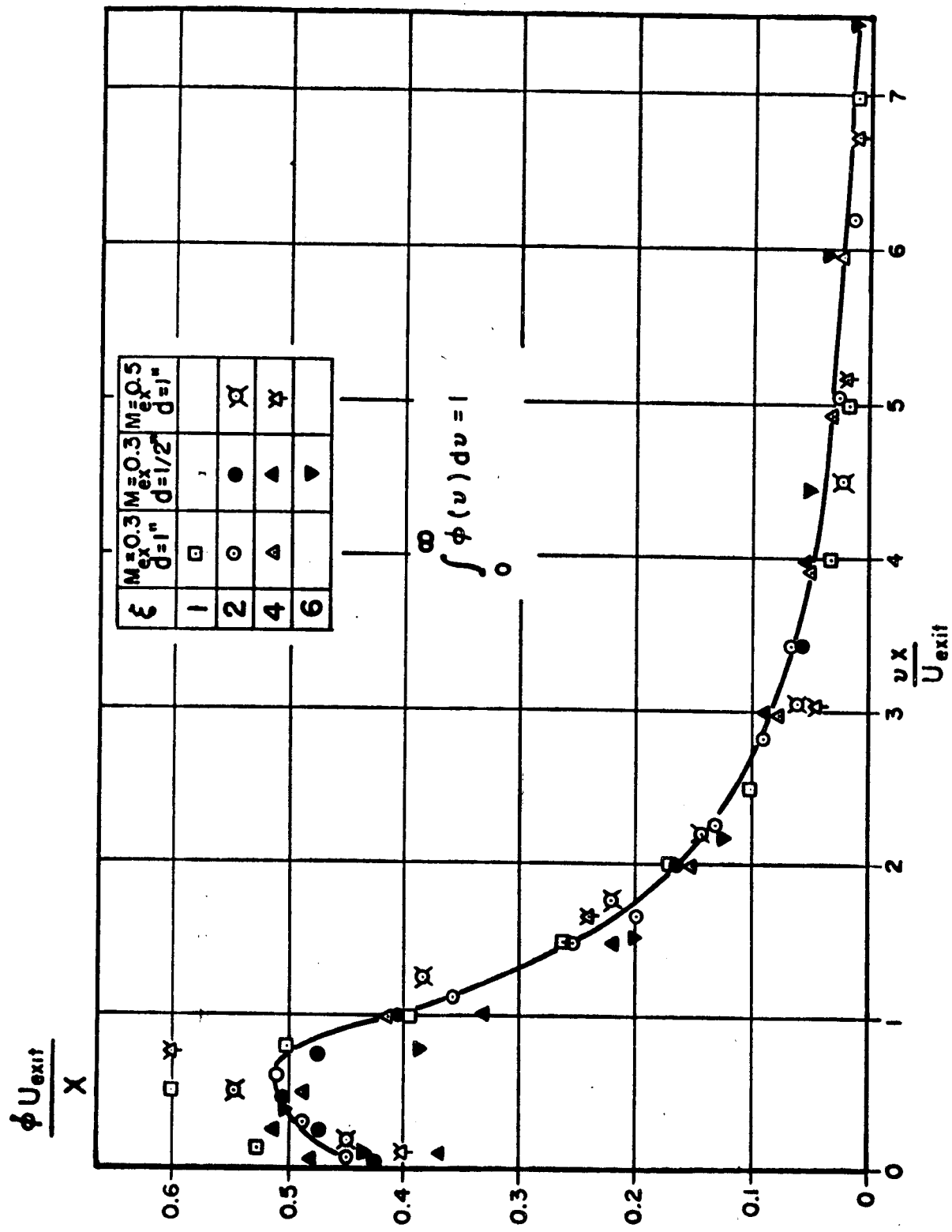

Figure 5. Power spectral density of u' as function of $\xi = \frac{x}{d}$ at $\frac{y}{d} = 1$ vs $\frac{x}{U_{exit}}$.

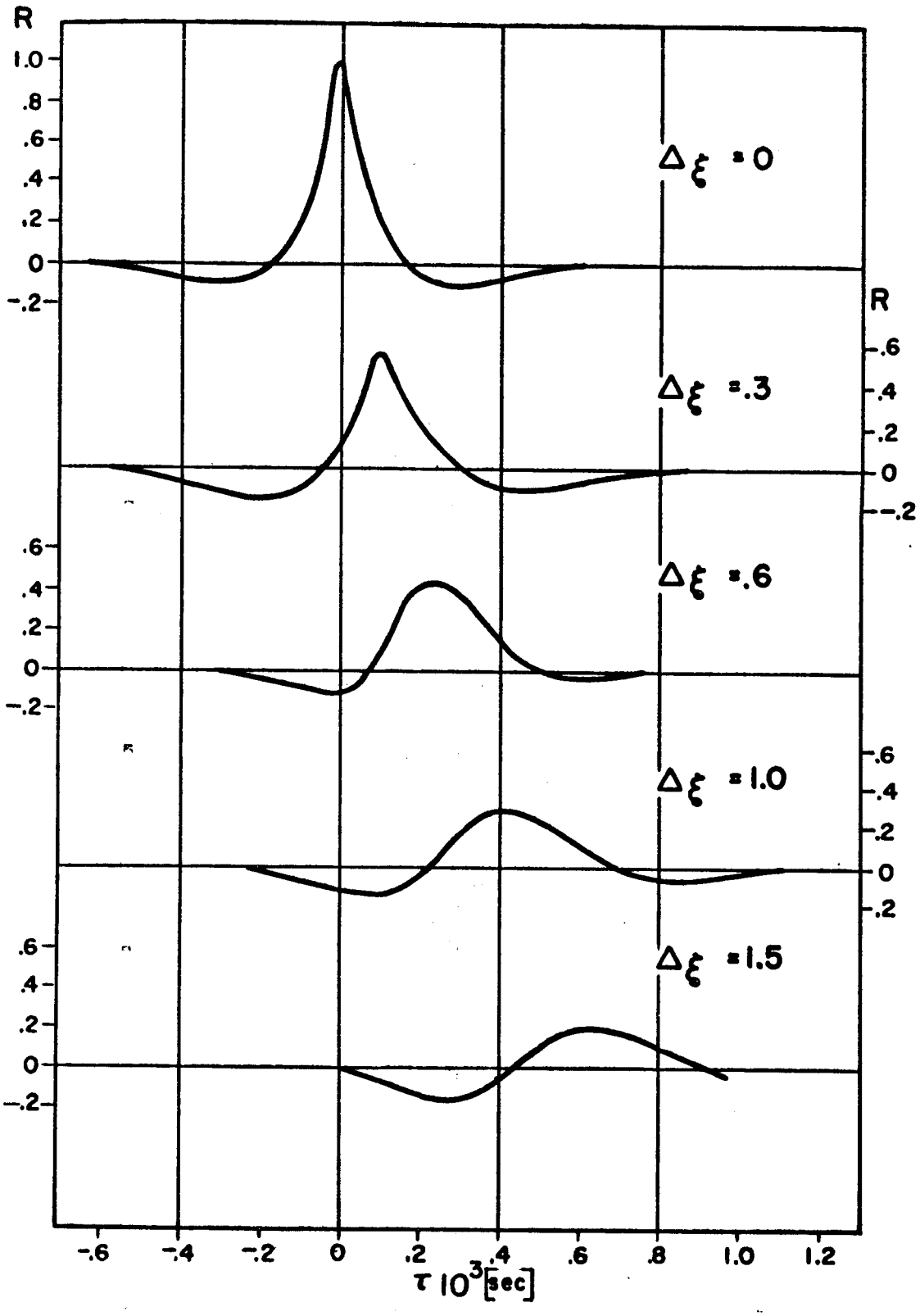

Figure 6. Space-time correlation coefficient R_{uu} of u' for $\xi = \frac{x}{d} = 2$, $\frac{y}{d} = 1$, d = 1", $M_{exit} = .3$ vs $\xi = \frac{x}{d}$ and τ .

$$R_{uu}(\xi, \Delta\xi, \tau) = \frac{\langle u'(\xi, t)\, u'(\xi+\Delta\xi, t+\tau)\rangle}{\bar{u}(\xi)\quad \bar{u}(\xi+\Delta\xi)}$$

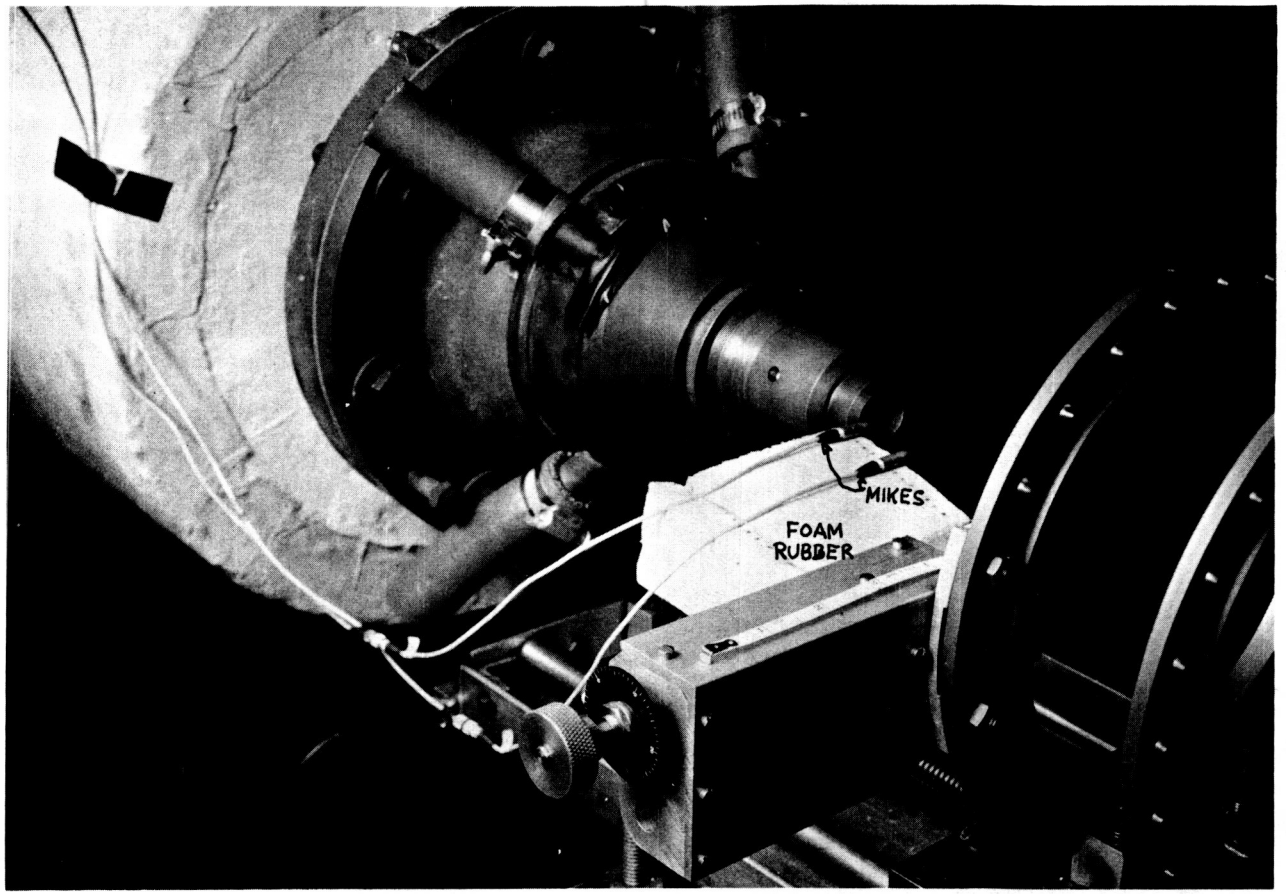

Figure 7. Microphone arrangement for near field measurements.

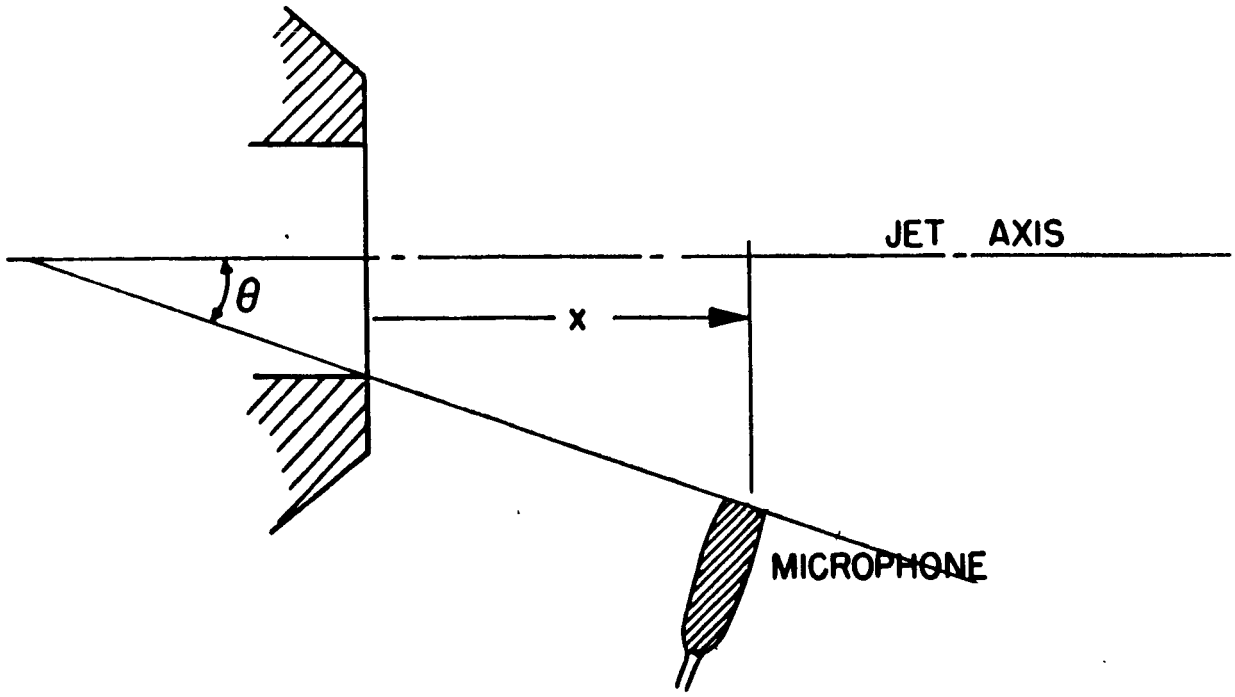

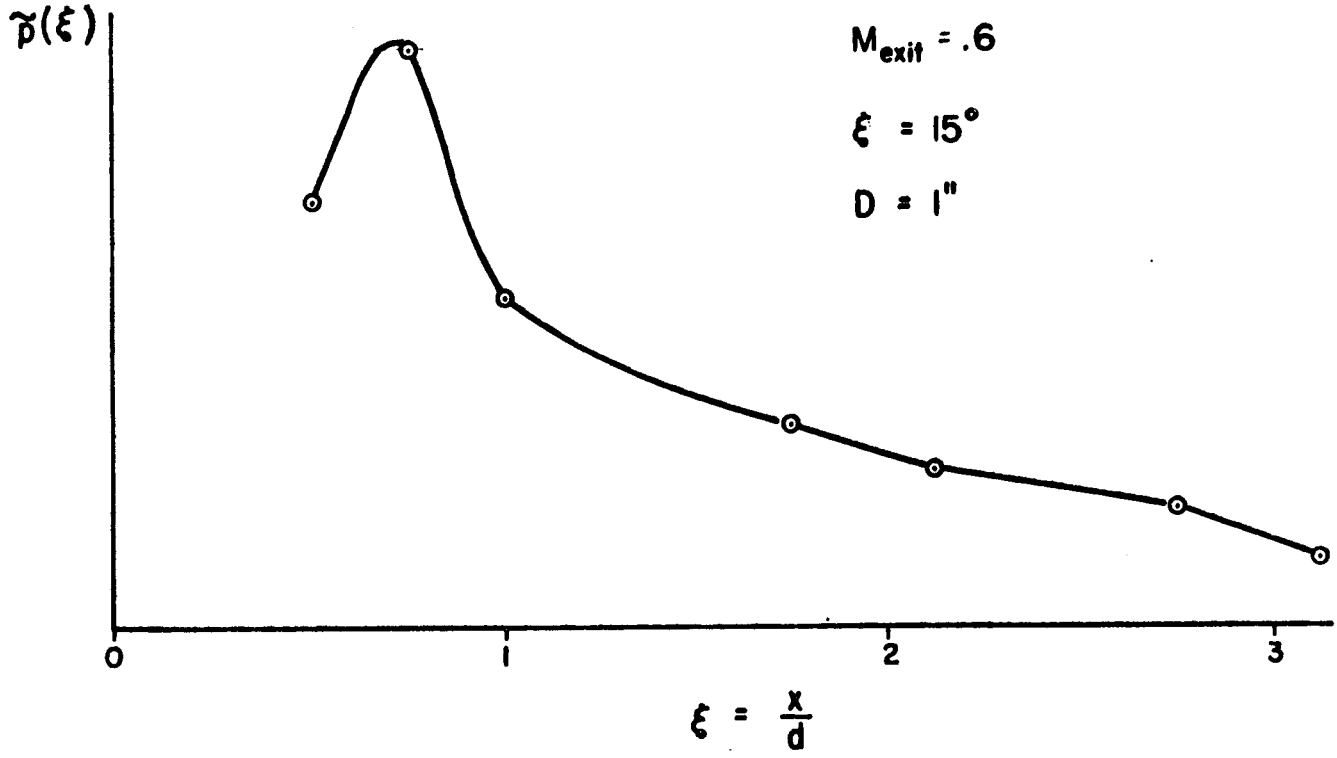

Figure 8. Variation of rms pressure fluctuation with distance along the jet.

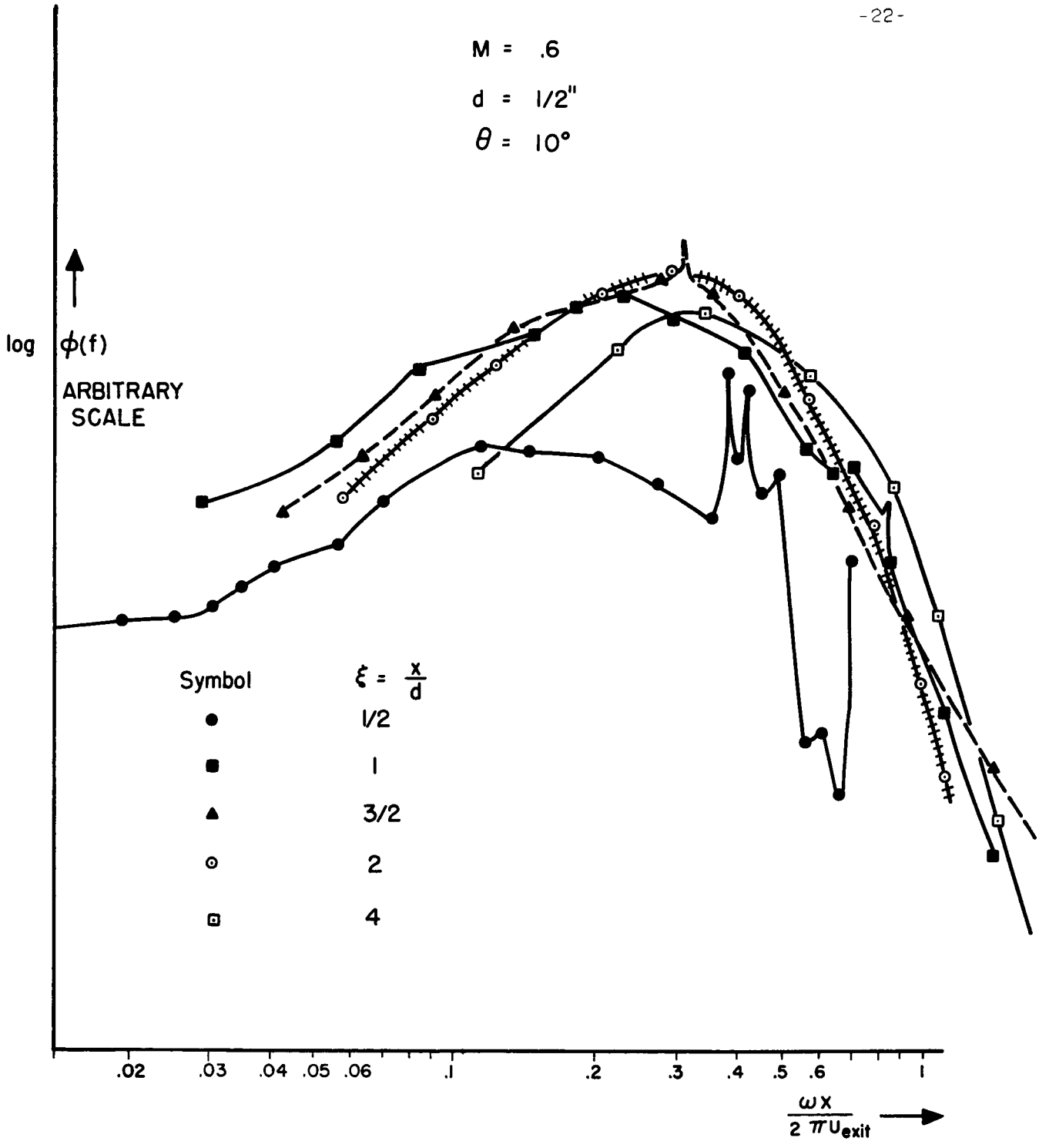

Figure 9. Near field pressure spectra at several streamwise locations.

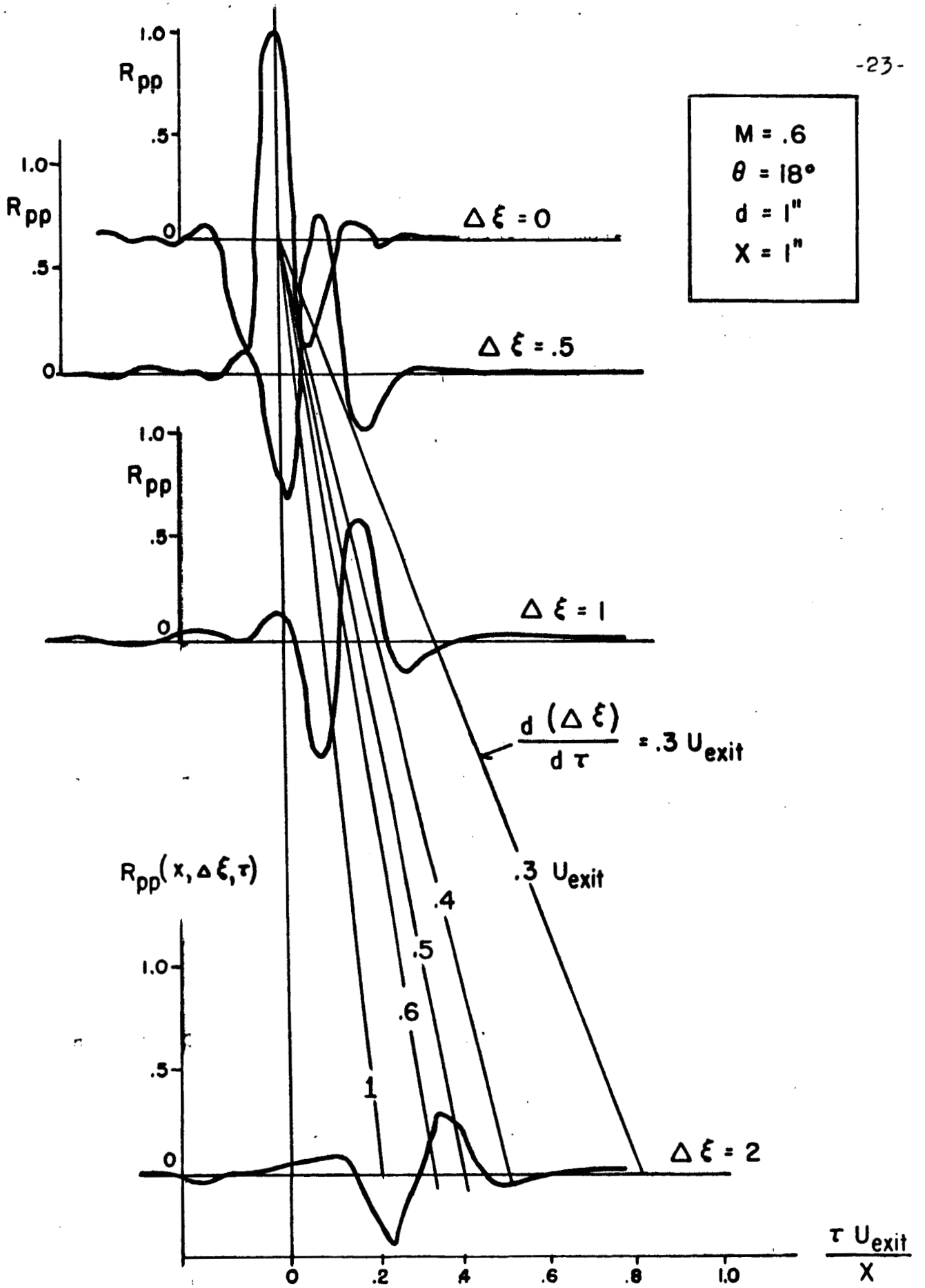

Figure 10. Space-time correlations of near field pressures.

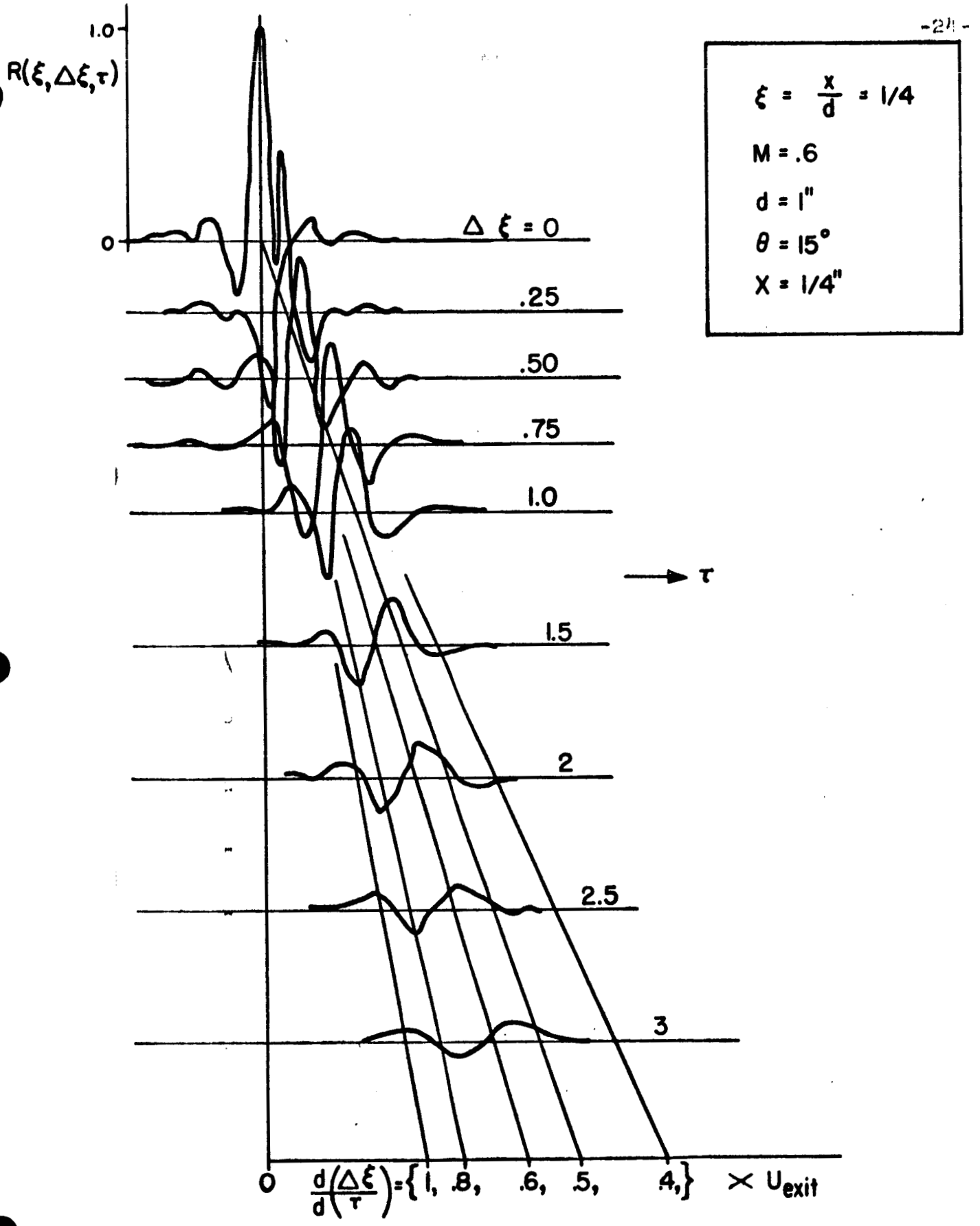

Figure 11. Space-time correlations of near field pressures.

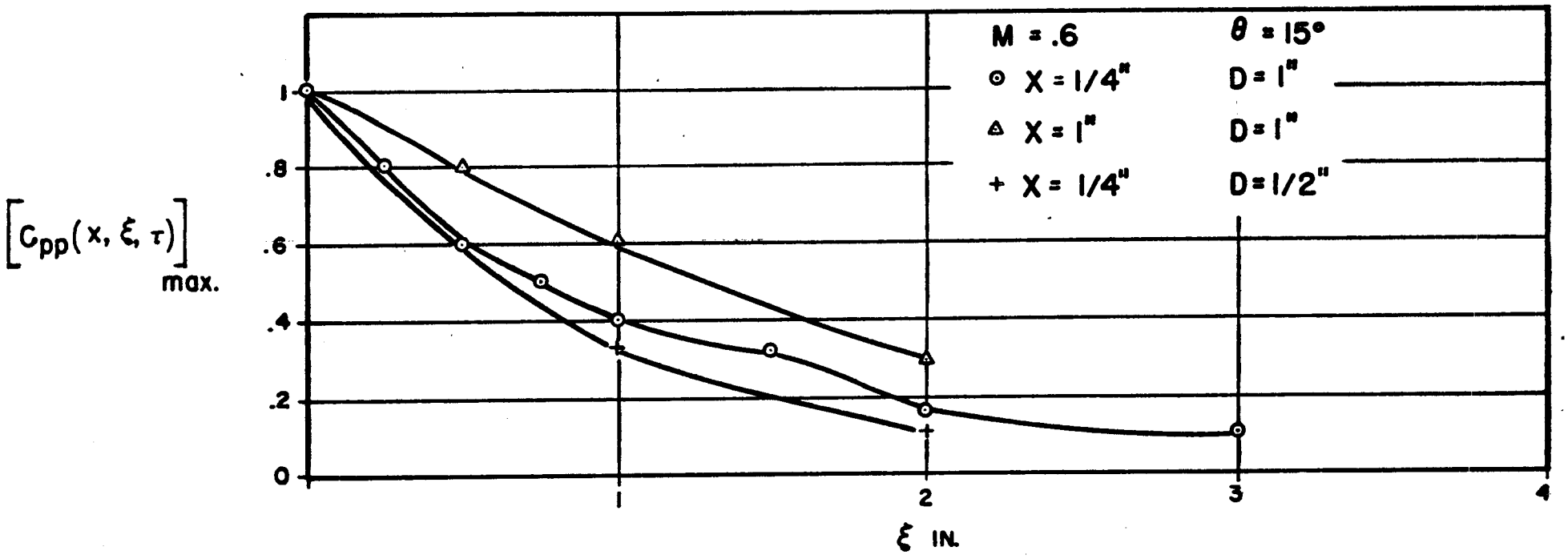

Figure 12. Variation of correlation coefficient with streamwise position.

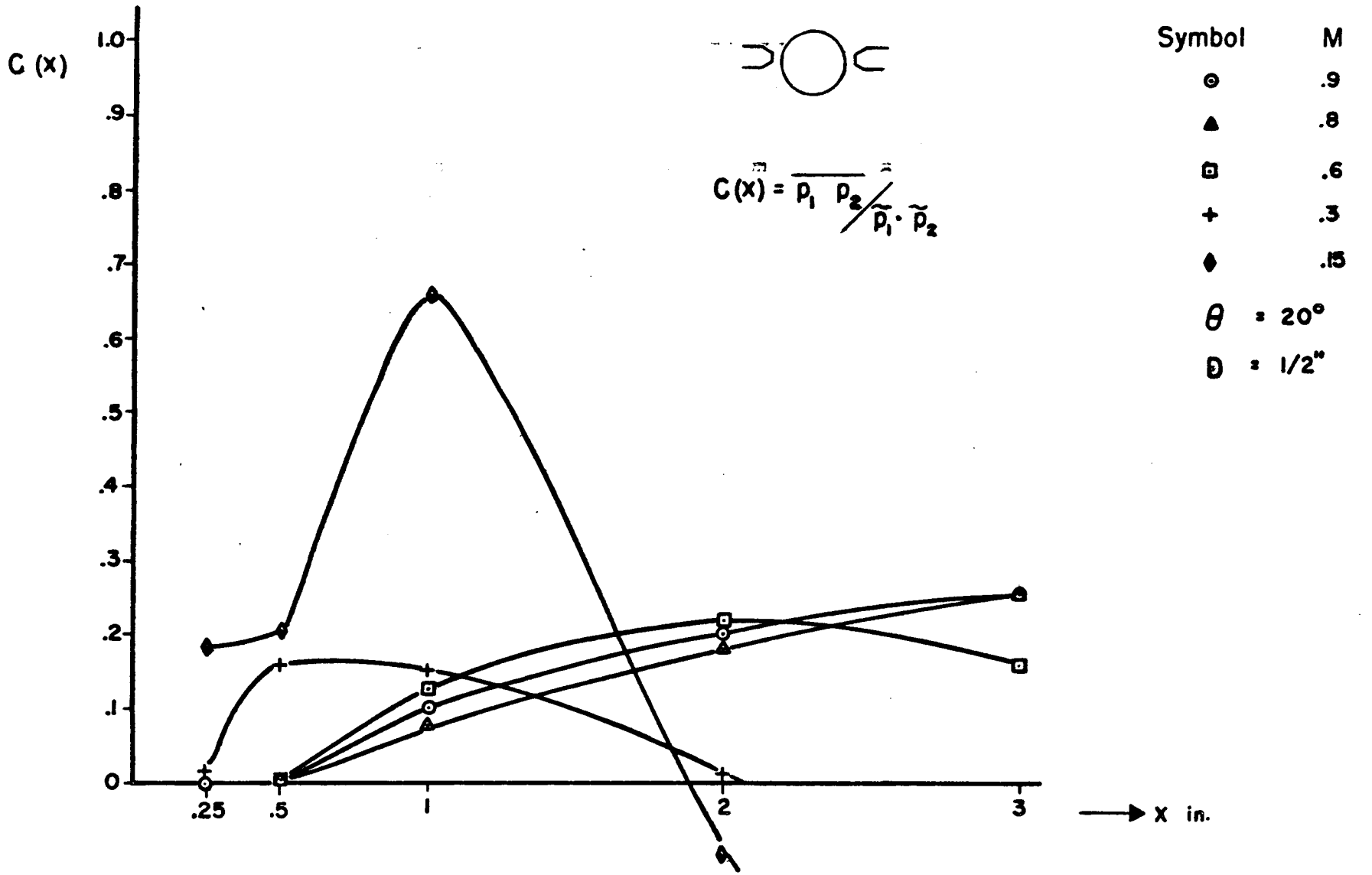

Figure 13. Cross-correlation across a jet diameter.

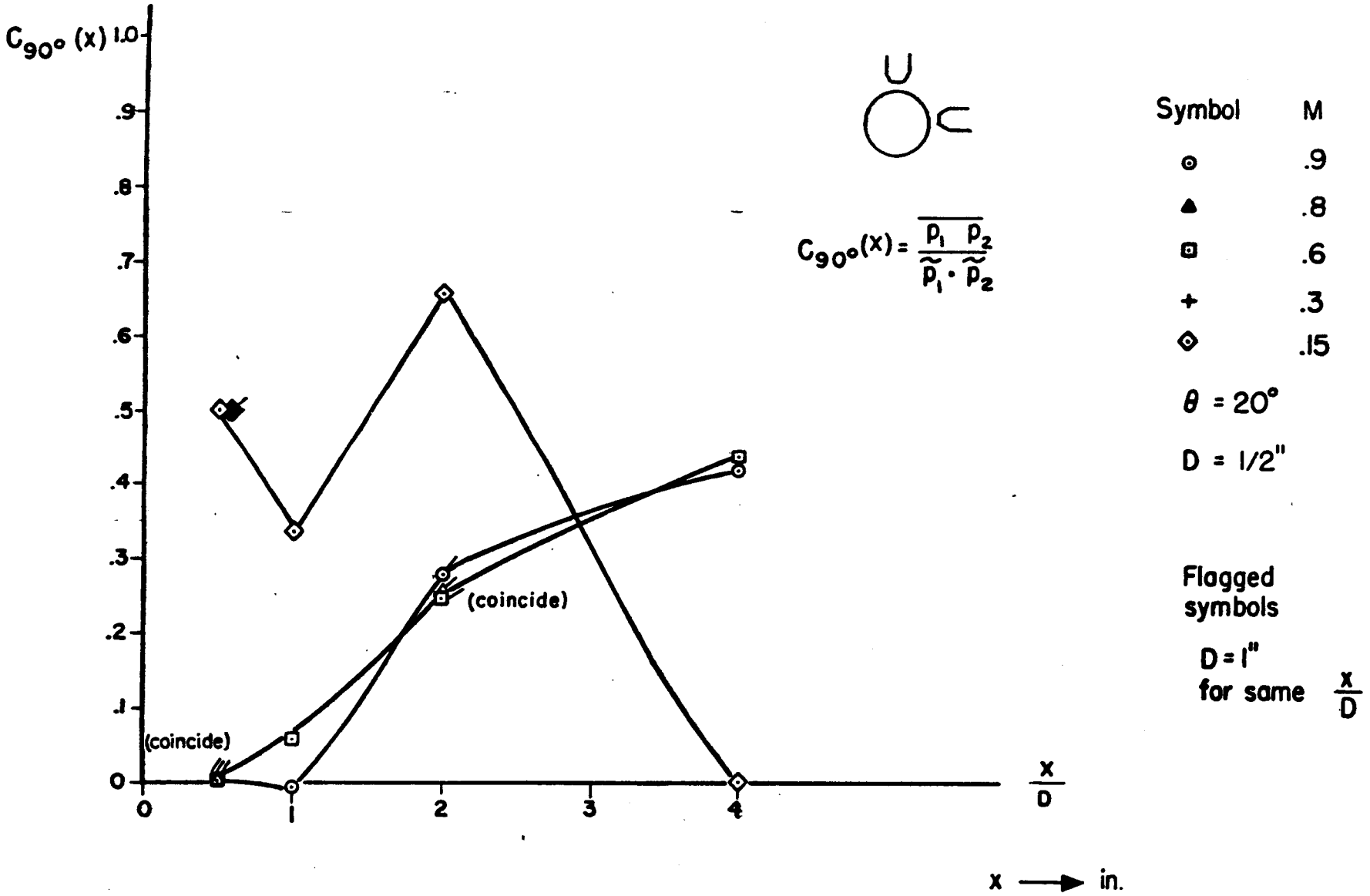

Figure 14. Cross correlation between points separated by 90° around the jet circumference.

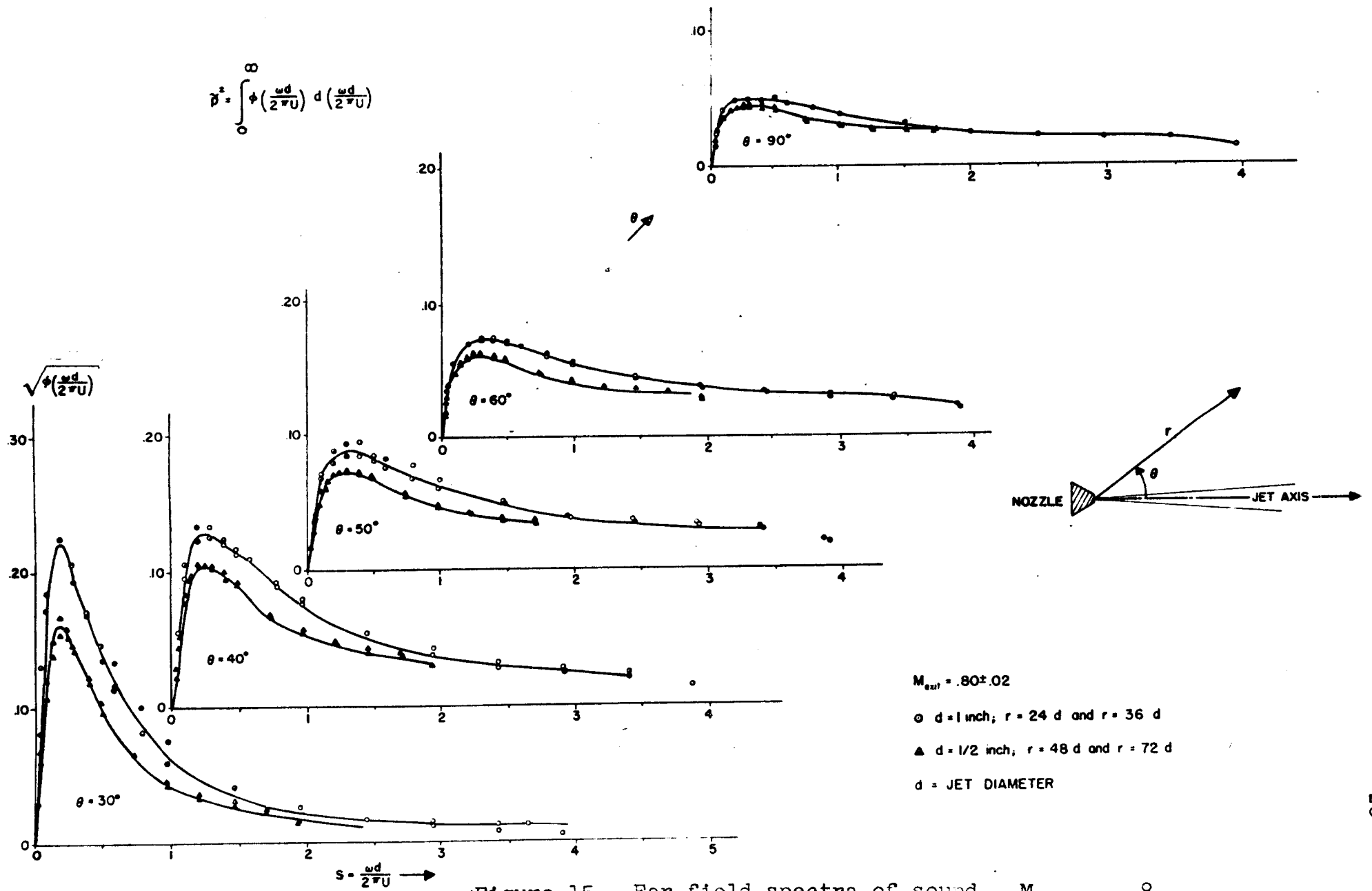

Figure 15. Far field spectra of sound. M_{exit} = .8.